EPJ Web of Conferences **63**, 02016 (2013)
DOI: 10.1051/epjconf/ 20136302016

Fission fragment mass and angular distribution in ^{6,7}Li+^{235,238}U reactions

S. Santra[1,a], A. Parihari[2], N. L. Singh[2], B. K. Nayak[1], B. R. Behera[3], K. Mahata[1], K. Ramachandran[1], Varinderjit Singh[3], A. Pal[1], R. Chakrabarti[1], S. Appannababu[1], R. Tripathi[4], S. Sodaye[4], P. Sugathan[5], A. Jhingan[5], E. Prasad[6], K. S. Golda[5], D. Patel[2], and S. Kailas[1]

[1] *Nuclear Physics Division, Bhabha Atomic Research Centre, Mumbai - 400085, India*
[2] *Department of Physics, The M. S. University of Baroda, Vadodara - 390002, India*
[3] *Department of Physics, Panjab University, Chandigarh - 160014, India*
[4] *Radio Chemistry Division, Bhabha Atomic Research Centre, Mumbai - 400085, India*
[5] *Inter University Accelerator Centre, Aruna Asaf Ali Marg, New Delhi - 110067, India*
[6] *Department of Physics, Central University of Kerala, Kasaragod, Kerala - 671123, India*

Abstract.
Fission fragment (FF) angular distributions for ^{6,7}Li+^{235,238}U reactions and mass distributions for ^{6,7}Li+^{238}U reactions have been measured at energies near and above the Coulomb barrier. The angle integrated fission cross sections for ^{6}Li induced reactions at sub-barrier energies are found to be higher than ^{7}Li induced reactions possibly due to larger contribution of breakup induced fission in case of the former compared to the latter. The FF anisotropy for ^{6,7}Li+^{235}U was found to be smaller than ^{6,7}Li+^{238}U, manifesting the effect of target ground state spin. The statistical saddle point (SSP) model predictions were found to be consistent with the measured FF anisotropy for ^{6,7}Li+^{235}U, however they were under-estimated for ^{6,7}Li+^{238}U particularly at lower energies. Observation of larger FWHM of FF folding angle distribution and sharp increase in peak to valley ratio for FF mass distribution with the decrease in bombarding energy in ^{6,7}Li+^{238}U reactions confirms the presence of breakup induced fission.

1 Introduction

The fission fragment (FF) mass and angular distributions provide a lot of information about the structure and reaction mechanism involving two interacting nuclei [1]. The breakup of weakly bound projectiles like ^{6,7}Li is expected to play an important role in modifying the energy dependent behavior of different observables like FF angular anisotropy and FF mass distribution [2, 3]. Due to low breakup threshold, the projectile ^{6}Li(^{7}Li) can breakup into α and $d(t)$ and one of these breakup fragments may get captured by the target forming compound nucleus (CN) which finally fissions into two fragments. Since the breakup fragment carries only a fraction of the total momentum of the projectile to the target, the compound nucleus formed by the capture of one of these fragments (incomplete fusion, ICF) acquires lower excitation energy compared to the one formed by complete capture of the projectile by the target (i.e. complete fusion, CF). The change in CN excitation energy may have effects on several observables as follows.

(i) *FF angular anisotropy:* It's value depends upon the variance of the K-distribution (K_o^2) of the CN (where K is the projection of the total angular momentum on the deformation axis). The value of K_o^2 is directly proportional to the temperature of the compound nucleus when it fissions into two fragments. Thus a significant contribution from breakup fragment induced fission may lead to an appreciable change in CN temperature which in turn will change the value of FF angular anisotropy.

(ii) *FF folding angle:* It is known that the folding angle of two fission fragment depends on the momentum transfer by the projectile to the target. So, a different momentum transfer which is associated with the incomplete fusion-fission (compared to complete fusion-fission) is expected to change the mean folding angle of the measured fission fragments. The combination of CF-fission and ICF-fission will result in broadening the full width at half maximum (FWHM) of the FF folding angle distribution.

(iii) *FF mass distribution:* The peak to valley ratio (P/V) of the double humped FF mass distribution is a measure of the degree of nuclear heating in the CN. Therefore, any change in the CN excitation energy due to contribution from the projectile breakup fragment induced fission would lead to a change in the value of P/V. So, one can also look into the effect of projectile breakup on the FF mass distribution by comparing its double humped structure with the ones obtained by n or p induced fission reactions involving similar compound nucleus.

To investigate all the above effects we carried out several measurements on the FF angular distribution for

[a] e-mail: ssantra@barc.gov.in

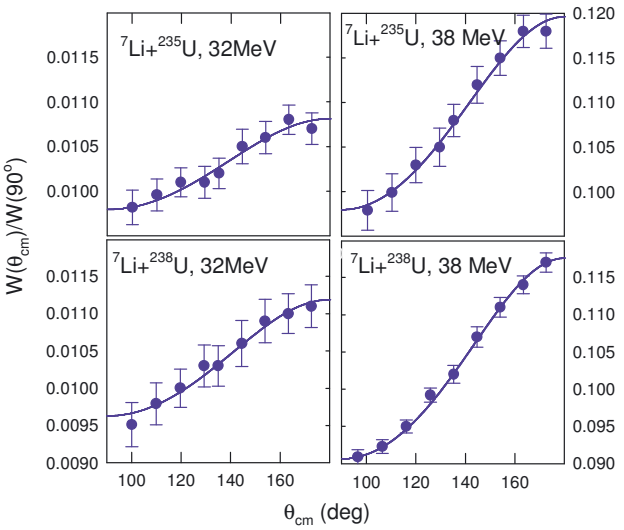

Figure 1. (Color online) Typical fission fragment angular distributions for ^{7}Li+^{235,238}U reactions at energies 32 MeV and 38 MeV. Solid lines correspond to the fit using the standard expression for FF angular distribution [4].

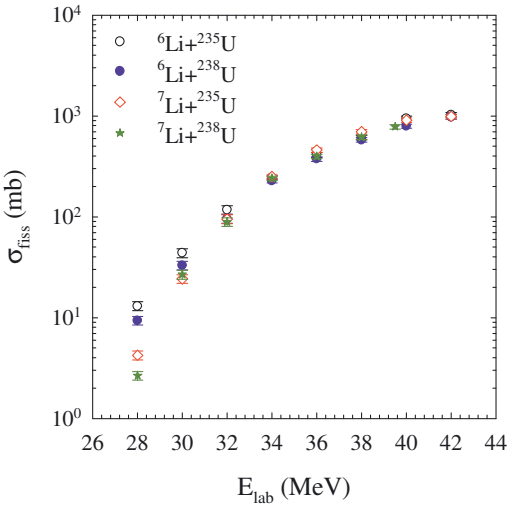

Figure 2. (Color online) Angle integrated fission excitation functions for ^{6,7}Li+^{235,238}U reactions, showing larger cross sections for ^{6}Li induced reactions (compared to ^{7}Li) at sub-barrier energies.

^{6,7}Li+^{235,238}U and mass distribution for ^{6,7}Li+^{238}U reactions. In addition to the projectile breakup effect, the effect of target spin was also investigated while comparing the FF angular anisotropy for ^{6,7}Li+^{235}U reactions with those for ^{6,7}Li+^{238}U reactions.

In this paper, we present the measurements for FF mass and angular distribution for ^{6,7}Li+^{235,238}U reactions. Details of the measurements for FF angular distributions and their results along with theoretical calculations are given in Section 2. Similarly, the measurements and the results on FF mass distributions are described in Section 3. Finally the results are summarized in section 4.

2 Fission fragment angular distribution

2.1 Experimental Details

Fission fragment angular distribution measurements were carried out using the 14 UD BARC-TIFR pelletron accelerator at Mumbai. Beam (^{6,7}Li) energies between 28 to 40 MeV in the step of 2 MeV have been used. Targets of ^{235,238}U of thickness $\sim 280\,\mu g/cm^2$ were prepared by electro deposition on $\sim$ 800 $\mu g/cm^2$ Al foil (which was used as a backing). The FFs were detected using five telescopes ($\Delta E - E$) of silicon surface barrier detectors of thickness $12-15\mu m$ for ΔE and $300-1000\mu m$ for E. Two Si surface barrier detectors, one kept at 15^o and another kept at 50^o were used as monitors for absolute normalization of fission cross sections. Contributions of the elastically scattered particles from Al backing was estimated by independent measurements using pure Al target of same thickness as in the backing. Typical fission fragment angular distributions for ^{7}Li+^{235,238}U reactions along with the theoretical fits at energies of 32 MeV and 38 MeV are shown in Fig. 1.

The measured FF angular distributions in center of mass W(θ) were fitted with the standard expression for angular distribution by Vandenbosch [4] to determine the anisotropies, $A = W(180^0)/W(90^0)$.

2.2 Fission cross sections and FF angular anisotropy

The total fission cross section (σ_{fiss}) was obtained by integrating the measured FF angular distribution at each beam energy. The fission excitation function for all the ^{6,7}Li+^{235,238}U reactions, as shown in Fig. 2, are found to be similar at above-barrier energies. However, at sub-barrier energies, the fission cross sections for ^{6}Li induced reactions (represented by hollow and filled circles) were found to be much higher than those for ^{7}Li induced reactions (represented by diamond and stars) which are consistent with the observation made by Freiesleben *et al.* [2]. Since the breakup threshold of ^{6}Li is lower compared to ^{7}Li, a larger contribution of breakup induced fission seems to be the primary reason for the observation of higher integrated fission cross sections for ^{6}Li induced reactions.

From the statistical model calculations it was observed that the fission probabilities of the CN formed by the above reactions are almost hundred percent. So, the fission cross sections were assumed to be same as fusion cross sections and they were compared with the fusion cross sections calculated by CCFULL code [5]. The standard coupling parameters available in the literature were used and the potential parameters were adjusted to set the Coulomb barrier that reproduces the measured fission excitation function. The average of the square of the angular momentum i.e., $< l^2 >$ for fusion was obtained at each energy and later used for anisotropy calculation described below.

FF anisotropies (A) were obtained from the measured FF angular distribution data and their corresponding fits for all the four reactions and are shown in Fig 3. It can be observed that the newly measured anisotropy for

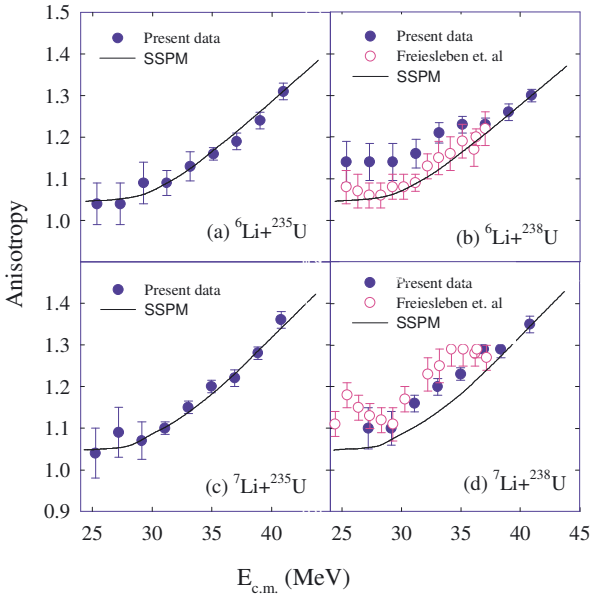

Figure 3. (Color online) Experimental (filled circles) and calculated fission fragment anisotropies as a function of centre of mass energy for (a) ^{6}Li + ^{235}U, (b) ^{6}Li + ^{238}U, (c) ^{7}Li + ^{235}U, and (d) ^{7}Li + ^{238}U reactions. Hollow circles represent the data from the literature [2]. Solid lines correspond to the SSPM calculations.

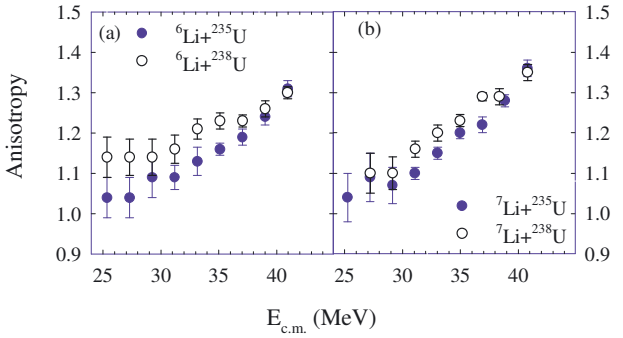

Figure 4. (Color online) Experimental fission fragment anisotropies as a function of centre of mass energy for (a) ^{6}Li + ^{235,238}U reactions and (b) ^{7}Li + ^{235,238}U reactions showing the effect of target dependence.

^{6,7}Li+^{238}U reactions has a non-smooth energy dependence behavior and is consistent with the previously measured data by Freiesleben *et al.* [2]. However, the absolute values of the present anisotropies are slightly different from the literature. The present FF anisotropies for ^{6}Li+^{238}U reaction were found to be slightly higher and for ^{7}Li+^{238}U reaction they were slightly smaller compared to the ones in the literature. The FF anisotropies for the two new systems i.e., ^{6,7}Li+^{235}U were found to have rather smooth behavior as a function of beam energy.

In Fig. 4, the FF anisotropies for the reactions involving same projectile but two different targets i.e., ^{235,238}U were compared. It can be observed that the anisotropy values for the reactions with ^{238}U targets are higher than the ones with ^{235}U targets. Such difference could be attributed to the difference in the target ground state spin, as all other relevant features (like deformation, mass, charge, etc.) are practically same.

The experimental anisotropies have also been compared with the predictions of the statistical saddle point model (SSPM). The value of anisotropy can be easily calculated by a simpler equation, $A = 1 + < l^2 > /4K_o^2$, approximated from the expression for fission fragment angular distribution given in [3], where, $< l^2 >$ is the mean squared angular momentum of the fissioning nucleus and $K_o^2 = (I_{eff}/\hbar^2)T$ is the variance of the K distributions. Here, I_{eff} is the effective moment of inertia and T (= $\sqrt{(E^*/a)}$ with $a = A_{CN}/9$ MeV^{-1}) is the saddle point temperature of the compound nucleus. Excitation energy E* at the saddle point is given by $E* = E_{c.m.} + Q - B_f - E_{rot} - E_n$ where, Q is the Q-value for the formation of the compound nucleus. The spin dependent fission barrier (B_f), ground state rotational energy (E_{rot}), and effective moment of inertia (I_{eff}) are calculated using the Sierk model [4]. E_n is the average energy removed by the evaporated neutrons from the compound nucleus. As mentioned earlier, the values of $< l^2 >$ were derived from the fit to σ_{fiss} with coupled-channels calculations.

The predicted values of anisotropy by SSP Model are shown in Fig. 3 as solid lines. The anisotropy values for ^{6,7}Li+^{235}U are consistent with SSPM calculation but for ^{6,7}Li+^{238}U they are larger compared to the SSPM calculations. There could be several factors that may lead to the above discrepancy in the anisotropy between theoretical calculation and experimental data for ^{6,7}Li+^{238}U reactions. For example, it is known that a large g.s. spin of the target or projectile can reduce the anisotropy at near- and sub-barrier energies and on the other hand a reduction in the variance of the K-distribution due to pre-equilibrium fission contribution can increase the anisotropy. Similarly, a large contribution of breakup induced fission can lead to a reduction in CN temperature which in turn reduces the value of K_o^2 and hence increases the anisotropy. Therefore the above discrepancy between theory and experiment could be due to a combined effect of (a) large difference in ground state spin of the targets (b) change in the K-distributions due to pre-equilibrium fission contribution and (c) reduction in average compound nucleus excitation energy due to breakup induced fission contribution. Further investigation to find the contribution from pre-equilibrium fission and breakup induced fission is needed to understand the above difference between the SSP model and experimental data for all the reactions at different energies.

3 Fission fragment mass distribution

3.1 Measurements

The experiment was performed using ^{6,7}Li beam from the 15-UD pelletron facility in Inter University Accelerator Centre, New Delhi. The ^{238}U target of thickness ~ 100 μg/cm^2 sandwiched between two layers of ^{12}C of thickness ~ 15 μg/cm^2 was used. Two multi-wire proportional counter (MWPC) detectors were used to detect fission

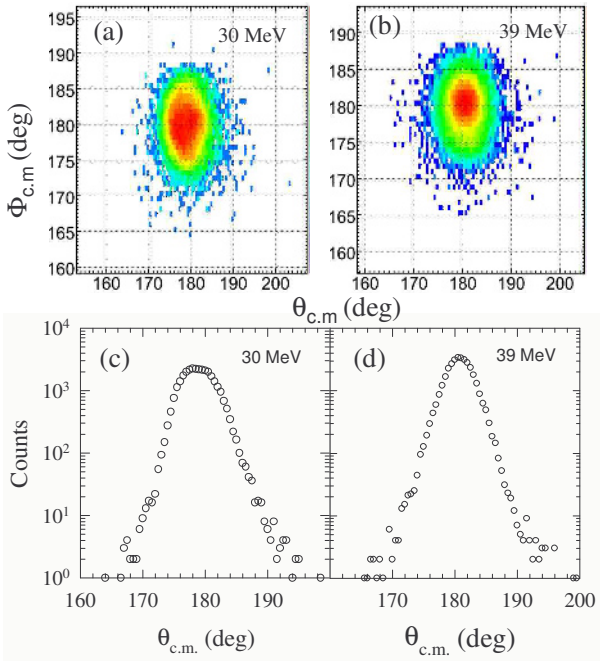

Figure 5. (Color online) Fission fragment folding angles distributions (FFFAD) in the reaction plane ($\theta_{c.m.}$) versus out of the plane ($\phi_{c.m.}$) for ^{6}Li beam energies of (a) 30 MeV and (b) 39 MeV. Respective projections on reaction plane are shown in (c) and (d) showing the difference in FWHM of the FFFAD.

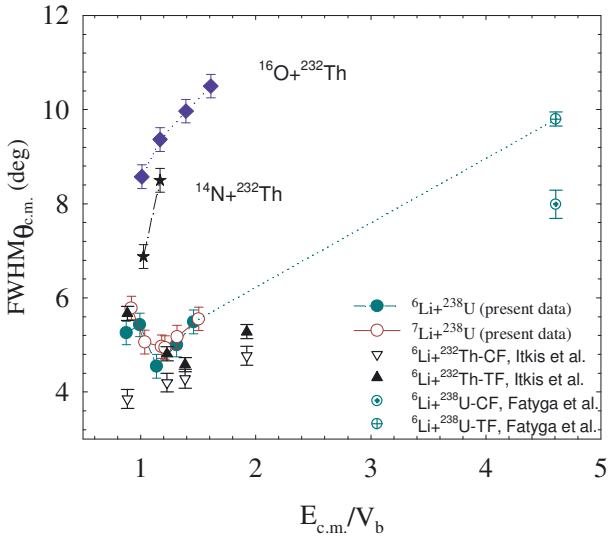

Figure 6. (Color online) Full width at half maximum (FWHM) of FFFAD as a function of energy normalized to Coulomb barrier ($E_{c.m.}/V_b$).

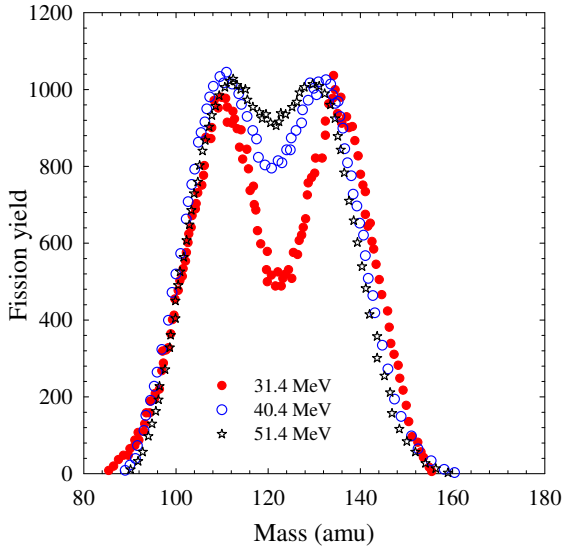

Figure 7. (Color online) Yield of fission fragments as a function of mass obtained from the reaction ^{7}Li+^{238}U at beam energies of 31.4 (filled circles), 40.4 (hollow circles) and 51.4 MeV (stars), showing the change in the shape of mass distribution with energy.

fragments. Both the MWPCs have an active area of 20x10 cm^2 and provide position signals in horizontal (X) and vertical (Y) planes, timing signal for time of flight measurements and energy signal giving the differential energy loss in the active volume. The start of the timing was taken from a small area (3.7 x 3.7 cm^2) transmission type fast timing multi-wire proportional counter and the stop was taken from the large area MWPCs. The combination of small MWPC and any one of the large MWPCs provide absolute timing of the fission fragments. Time of flight signal in combination with differential energy loss signal gives a clean separation of fission fragments from projectile and target like particles.

Fig. 5 shows typical fission fragment folding angles distributions (FFFAD) in the reaction plane ($\theta_{c.m.}$) versus out of the plane ($\phi_{c.m.}$) for ^{6}Li at two energies and their respective projections on reaction plane.

3.2 FF folding angle distribution

In Fig. 6, full width at half maximum (FWHM) of FFFADs for ^{6,7}Li+^{238}U systems have been compared with the ones with tightly bound projectiles. It can be observed that the FHWM at energies above the Coulomb barrier for ^{16}O+^{232}Th[8] and ^{14}N+^{232}Th[9] systematically decreases with lowering the beam energy. As the energy increases, the CN excitation energy increases and the probability of more and more number of neutron or charged particle evaporation increases. This leads to an increase in the width of the folding angle distribution. But the energy dependence behavior of the FWHM for the present systems is quite different. The value of the FWHM first decreases and then increases with energy. The increase in the FWHM at lower energies is possibly due to the large contribution of breakup fragment induced fission compared to complete fusion-fission.

3.3 Peak to valley ratio of FF mass distribution

Fig. 7 shows typical yield of fission fragments of different masses detected in the ^{7}Li+^{238}U reaction at three energies: 31.4, 40.4 and 51.4 MeV. It can be observed that the double humped structure in the mass distribution is more

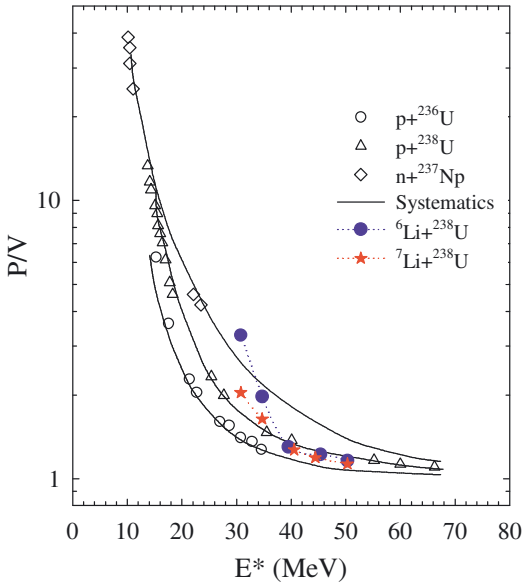

Figure 8. (Color online) Ratio of peak to valley (P/V) of the fission fragment mass distribution for ^{6,7}Li+^{238}U along with literature data for *n* and *p* induced fission of the actinides. Results of systematics are shown as solid lines. See text for details.

prominent at 31.4 MeV compared to that at 51.4 MeV. At higher energies, it gradually approaches to become a single hump with symmetric mass distribution. The mass distributions obtained from the measured fission data for ^{6}Li+^{238}U reaction at slightly different energies (but with same excitation energies) also showed a similar behavior.

The ratio of the peak to valley of the fission fragments mass distribution, that gives the information about the nuclear heating, are calculated for ^{6,7}Li+^{238}U reactions at different energies and plotted in Fig. 8 as filled circles and stars respectively. The P/V values of the mass distributions corresponding to *p* and *n*-induced fissions of Uranium and Neptunium targets along with the calculations from systematics [7] are also shown in the above figure to compare with the present results. It is interesting to observe that although the P/V values for ^{7}Li+^{238}U (stars) follows the trend similar to the systematics in the measured energy range, the values for ^{6}Li+^{238}U (filled circles) at lowest two energies are very large compared to the rest of the systems. The larger value of P/V for ^{6}Li+^{238}U implies that the average excitation energy of the compound nuclei formed in this reaction must be smaller, due to incomplete fusion (ICF) contribution, than the one we have calculated assuming complete fusion only. However, for ^{7}Li+^{238}U, the ICF contribution seems to be much less compared to the case of the former. This observation was supported by comparing the angle integrated fission cross sections, where it was found that the fission cross sections at sub-barrier energies for ^{6}Li induced reactions are much larger than the ones for ^{7}Li induced reactions implying larger contribution of breakup induced fission in case of the former due to lower breakup threshold.

4 Summary

Fission fragment mass distributions for ^{6,7}Li+^{238}U and angular distributions for ^{6,7}Li+^{235,238}U reactions are measured at energies around the Coulomb barrier. Due to larger ground state spin for ^{235}U target, the FF anisotropy in ^{6,7}Li+^{235}U reactions at and below the Coulomb barrier energies was found to be smaller compared to those for ^{6,7}Li+^{238}U. No appreciable difference in FF anisotropy was observed between ^{6}Li and ^{7}Li induced reactions involving a particular target. SSPM calculations reproduce the anisotropy for ^{6,7}Li+^{235}U but under-predict it for ^{6,7}Li+^{238}U which probably manifests the combined effect of pre-equilibrium fission, breakup induced fission and target spin difference. Angle integrated fission cross sections for ^{6}Li+^{235,238}U at sub-barrier energies were found to be higher than ^{7}Li+^{235,238}U implying more contributions from breakup/transfer induced fissions for the former compared to the later. Energy dependence of the FWHM of the FF folding angle distribution for ^{6,7}Li+^{238}U shows a behavior different from those involving tightly bound projectiles. At energies just below the Coulomb barrier, the FWHM of the FF folding angle distribution increases unlike for the case of ^{14}N+^{232}Th or ^{16}O+^{232}Th where it decreases. With the decrease of CN excitaion energy, the P/V value of the FFMD for ^{6}Li+^{235,238}U increases much sharply than ^{7}Li+^{235,238}U showing the effect of projectile breakup threshold or d/t transfer Q-value.

Acknowledgements

One of the authors (A. Parihari) acknowledges the financial support from the UGC-DAE CSR, Kolkata Centre for carrying out these investigations.

References

[1] S. Kailas, Physics Reports **284** (1997) 381.
[2] H. Freiesleben *et al.*, Phys. Rev. C **12** (1975) 42.
[3] I. M. Itkis et al., Phys. Lett. **B 640** (2006).
[4] R. Vandenbosch and J.R. Huizenga, Nuclear Fission (Academic press, New York, 1973).
[5] K. Hagino, N. Rowley, and A. T. Kruppa, Comput. Phys. Commun. **123**, 143 (1999).
[6] A. J. Sierk, Phys. Rev. **C 33**, 2039 (1986).
[7] D. M. Gorodisskiy *et al.*, Ann. Nucl. En. **35** (2008) 238.
[8] R.K. Choudhury *et al.*, Phys. Rev. C **60** (1999) 054609.
[9] B.R. Behera *et al.*, Phys. Rev. C **69** (2004) 064603.